論　　文

Step and Flash Imprint Lithography: A Technology Review

T. Bailey, B. J. Choi, M. Colburn, A. Grot[a)], M. Meissl, M. Stewart,
J. G. Ekerdt, S. V. Sreenivasan, and C. G. Willson

Texas Materials Institute,The University of Texas at Austin, Austin, Texas

[a)]Agilent Technologies, Palo Alto, CA

翻訳：蔡 兆申　日本電気(株)

The development of imprint lithography is an attempt by researchers to meet or exceed the size targets outlined in the SIA roadmap for semiconductors, while circumventing the expensive exposure sources and optics required by more conventional next generation lithographies, such as extreme UV, electron projection, and X-ray lithographies. There are promising applications in addition to the semiconductor arena, such as micro-electromechanical devices (MEMs), micro-optics, and patterned storage media. Imprint lithography has the advantage that it uses fundamental fluid displacement principles to define a pattern, rather than image reduction with diffraction corrections, but the temperatures required by the more traditional micromolding or hot embossing techniques may present insurmountable obstacles in overlay alignment accuracy, and for applications requiring high throughput.
Step and Flash Imprint Lithography (SFIL), being developed primarily at the University of Texas at Austin, overcomes these issues by using a rigid, UV-transparent imprint template, and a bilayer resist scheme composed of an organic planarizing layer and a low viscosity, UV-curable organosilicon solution for imprint imaging. We describe the technology fundamentals here.
We demonstrate a durable, low surface energy template release coating, a UV-curable organosilicon etch barrier that cures with low dosage, and the equipment that allows for the high-precision orientation of the template/substrate system necessary for imprint patterning. We have demonstrated printed features as small as 60 nm (not shown), compatibility with metal lift-off processing, functional optical devices including a micropolarizer array, and the ability to pattern high-aspect ratio, sub 0.25 micron features over a non-flat substrate.

概　要

SIAロードマップ上で予測されている微細な寸法目標を、大変高価である従来から研究されてきた次世代リソグラフィ（極UV、電子線投影、X線等）に頼らずに達成するため、インプリントリソグラフィ技術は研究されている。この技術は半導体LSI以外にもマイクロ電気機械システム（MEMS)、マイクロ光学、およびパターン化記憶媒体などへの応用が有望視されている。流体排出の基本原理を利用するインプリントリソグラフィは、像の縮小投影やそれに伴う回折ゆがみの修正等を一切必要としない利点がある。しかしインプリントリソグラフィ技術の中でも、より伝統的なマイクロ鋳造法(micromolding)や熱型押し法(heat embossing)などでは、目合わせ精度やスループットについて克服しがたい障害が存在する。しかし現在主にテキサス大学オースティン校で開発されつつあるステップ･アンド･フラッシュ　インプリントリソグラフィ（SFIL）と名づけた技術は、このような課題を克服できる。この技術では、UVに透明な硬質な型押しテンプレートと、有機平坦化層と低粘性でUV硬化するシリコン有機物溶液からなる二層レジストを使う。この詳細を以下に紹介する。

我々は、テンプレート切り離し用の耐久性のある低表面エネルギーコーティング、低ドーズで硬化するUV硬化性シリコン有機物エッチマスク、そしてインプリントに必要なテンプレート・基板システムの高精度位置制御を実現した。この技術で最小60nmの形状のプリント転写に成功した。そしてこの技術の金属リフトオフ法との両立性、マイクロ偏光器を含む機能性光学素子への応用、そしての高アスペクト比構造の凹凸基板上での0.25ミクロン以下パターニングを実証した。

1　Introduction

Optical lithography is being extended to pattern sub-wavelength features. A combination of improvements in optics, further reduction in wavelength, and introduction of more complex processes will enable printing features smaller than 100 nm. Unfortunately, the cost of exposure tools is increasing exponentially[1)]. The Semiconductor

Industry Association roadmap lists several next generation lithography (NGL) techniques based on ionizing radiation: X-ray, extreme UV (EUV), and direct-write e-beam. Each has its advantages and disadvantages, but all are expensive. We seek an inexpensive method of pattern generation capable of sub-100 nm resolution on silicon substrates. If it is to be significantly cheaper, such a process must, by necessity, be very different from those now contemplated.

Photolithography resolution is known to follow the well known relationship[2]:

$$R = \frac{k\lambda}{NA} \qquad (1)$$

where k is dependent on the system, which includes resist material contrast, λ is the wavelength of the light, and NA is the numerical aperture of the lens. These parameters are not relevant to imprint lithography because the technology does not use reduction lenses. Imprint Lithography has several competitive advantages to conventional optical lithography and NGLs. The resolution capabilities of imprint techniques in the sub 100 nm regime are well-documented[3, 4]. Imprint resolution appears to be limited only by the resolution of the template or mold topography. These templates are typically fabricated using imaging tools such as electron beam writers which provide high resolution but lack the throughput required be mass production. Imprint lithography is therefore takes advantage of the resolution offered by e-beam technology without compromising throughput.

2 Imprint Lithography

There are many imprint lithography techniques, all variations of a common theme. The basic premise is that a template or mold with a prefabricated topography is pressed into a displaceable material. That material takes on the shape of the master pattern defined in the template, and through some curing process is hardened into a solid. The process is by nature a contact patterning process which transfers patterns without scaling, and so there are common challenges to all of these imprint techniques, the foremost being the limitation of this technology by the imprint master resolution. Particle contamination is also a major concern, as it is with any contact lithography technique; imprint lithography faces the added challenge in that it is susceptible to particle contamination on the wafer backside as well as on the surface.

Imprint lithography techniques were systematically studied by researchers in 1990's[3-8]. The research is divided into two camps, one camp preferring imprinting into a thermoplastic or thermoset polymer, and the other imprinting into a ultraviolet light-curable material. Chou and coworkers[3, 9, 10] use an imprint technique based on embossing a thin film of poly(methyl methacrylate) (PMMA), or similar polymer, during a heating cycle that allows the film to conform to a template containing a topography. The group has become quite adept at producing structures that do not require overlay registration. Chou and coworkers have demonstrated high density magnetic storage disks[11] and high density compact disks[12], waveguide polarizers[13], photodetectors[14] and light-emitting structures[15], and field effect transistors[16] and single-electron transistor memory[17], none of which report significant overlay control.

Scheer and coworkers[8, 18] have also focused on high temperature imprint lithography, although their work is more related to the fundamentals of imprint patterning. The authors found that the process is limited by material transport, and that pressures of around 100 bar and temperatures 90 ºC above the polymer glass transition temperature are optimal for material displacement[8, 18]. These studies were performed using imprint molds with a global average pattern density near 50%, where "positive" pattern areas are defined to require less material displacement, and conversely for "negative" pattern areas. The authors conclude that regular repeating patterns and areas in positive tone are ideal for this type of patterning[8].

Jaszewski, *et al.*[7] have developed a "hot embossing" technique of patterning, which is fundamentally similar to the Chou[3] and Scheer[8] methods. The authors have demonstrated compatibility with metal lift-off techniques using titanium[7].

These three groups follow the same basic technology, that a polymer heated above its glass transition temperature (T_g) is imprinted with a mold. The system is cooled to below the T_g of the polymer while the mold is in contact, thus curing the shape of the imprint. Three issues pose serious challenges if this technique is to be used for semiconductor or optical devices that require layer-to-layer alignment: (i) heating cycles cause thermal expansion mismatch of template to substrate and are inherently slow relative to desired manufacturing throughput, (ii) non-transparent templates make layer-to-layer alignment difficult, and (iii) large applied pressures that are required to displace high-viscosity polymers such as PMMA cause mechanical distortion and introduce potential for catastrophic failure of

brittle underlying semiconductor materials. To address the thermal cycle issue, Chou's group has been working with a new set of polymers with lower glass transition temperatures that enable process temperatures to be lowered to 100 ºC [19]. The authors do not discuss, however, the details of the polymer composition. They have also developed customized alignment schemes to demonstrate course overlay with about 1 micron accuracy via a set of vernier patterns[20].

We have previously investigated the prospect of imprinting a silicon thermoplastic at elevated temperatures and pressures[4]. Our goal was to generate a bilayer structure analogous to that produced by bilayer or tri-layer lithographic processes[21]. An organic thermoset planarizing/transfer layer was coated on a silicon wafer and then cured. A thin layer of a silicon-containing thermoplastic was spin coated on the transfer layer. An etched polysilicon/silicon template was brought into contact with the coated substrate. This "sandwich" structure was then placed in a press and heated to 150 ºC under pressure for 15 minutes. An advantage of such a bilayer process is that one needs only to generate low aspect ratio features. These features can then be transferred through the transfer layer via an anisotropic O_2 reactive ion etching (RIE) process analogous to that used in bilayer lithography, to generate high aspect ratio, high-resolution images.

Some results from this compression molding process are shown in ***Figure 1***. The micrograph in ***Fig. 1(a)*** demonstrates the transfer of 2 µm grating features over a large area. The image in ***Fig. 1(b)*** illustrates a serious problem with this approach. Imprinting with varying pattern density results in incomplete displacement of the thermoplastic even at elevated temperature and high pressure for long periods of time. Partial pattern transfer, failure to displace material completely, release difficulties, and harsh process conditions seemed to limit the potential of this approach. Scheer, *et al*.[8] also have documented these problems with compression molding of PMMA derivatives. The use of high temperatures and high pressures would also severely complicate layer-to-layer alignment issues found in microelectronic device fabrication.

The second fundamental route to imprint lithography relies on curing a photosensitive material with ultraviolet light, rather than using the heated polymer method described above. This method has been used in the production of optical disks[22]. Philips Research has demonstrated a photo-polymer process which produces high-resolution polymer features[5]. In this process, a liquid acrylate formulation is photopolymerized in a glass template to generate the required topographical features. While the Philips process shows promise for creating high-resolution images, it does not produce high aspect ratio images, and the patterned acrylate polymers lack the etch resistance required for semiconductor manufacturing.

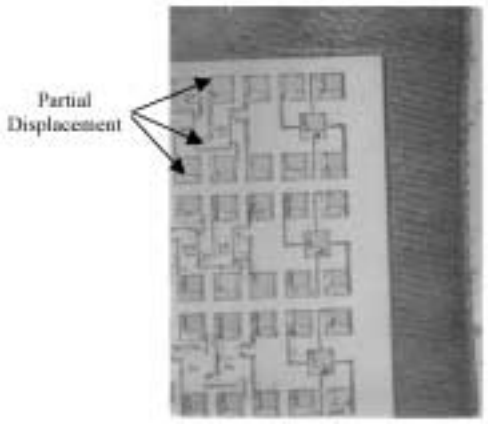

図1　インプリントリソグラフィ技術の初期のステップ･アンド･スクァッシュ(Step and Squish)法の結果の光学顕微鏡写真。パターン密度が不均一の場合、ポリマーが完全に排出されない現象が見られる。この方法はChou[3]やScheer[8]の方法の延長上にある技術であるがShaw等[21]に提案された二層レジスト法を使った。

Fig. 1 Results from "Step and Squish" imprint lithography, an early predecessor to the current technology. Optical micrograph of a pattern, showing partial displacement of polymer in a pattern with irregular pattern density. This was an extension of the methods of Chou[3] and Scheer[8], but using the bilayer resist scheme suggested by Shaw, *et al*.[21].

Because of our experience and that of others, we choose to refocus our efforts on a different technique that we call "Step and Flash Imprint Lithography."

3. Step and Flash Imprint Lithography

3.1 Overview

Step & Flash Imprint Lithography (SFIL) is a novel, high throughput, low cost approach to generating relief patterns with sub 100 nm line width. SFIL uses no projection optics, no lenses, and operates at room temperature; the process relies largely on chemical and low pressure mechanical processes to transfer patterns. SFIL is related to other micro-molding or imprint processes[3, 5, 6, 23, 24] in that all of these use the topography of a template to define the pattern created on a substrate. The two key differences between SFIL and other imprint lithography techniques are that this process is based on a low viscosity, photo-curable liquid, and SFIL uses a

transparent, rigid template. The low viscosity of the photo-curable liquid eliminates the need for high temperatures and pressures that can lead to substrate deformation, which can inhibit accurate overlay of layers in device fabrication. The rigid imprint template is transparent in order to allow the flood exposure of the photopolymer to achieve cure, and this combination of rigidity and transparency also enables optical layer-to-layer alignment error measurement for multilayer device fabrication.

The SFIL process flow is shown on the left side of ***Figure 2***. The right side of the figure is the process flow used in collaboration with Agilent Technologies, and will be discussed later. An organic transfer layer is spin-coated on a silicon substrate. A low viscosity, photopolymerizable, organosilicon solution is dispensed on the wafer in the area to be imprinted. A surface-treated, transparent template bearing relief structures of a circuit pattern is closely aligned over the coated silicon substrate. The template is lowered in contact with the substrate, displacing the etch barrier to fill the imprint field. The structure is irradiated with ultraviolet light through the backside of the template, curing the photopolymer. The template is then separated from the substrate leaving a relief image on the surface of the coated substrate. A short halogen etch is used to break through the undisplaced etch barrier material, exposing the underlying transfer layer. An oxygen RIE amplifies the aspect ratio of the imprinted image. The imprinting process is conducted at room temperature, and since the template is transparent, all of the alignment schemes that have been used successfully in mask aligners, photolithography steppers and scanners can be implemented without difficulty. The process is simple in concept, but every step in the process presents interesting challenges in

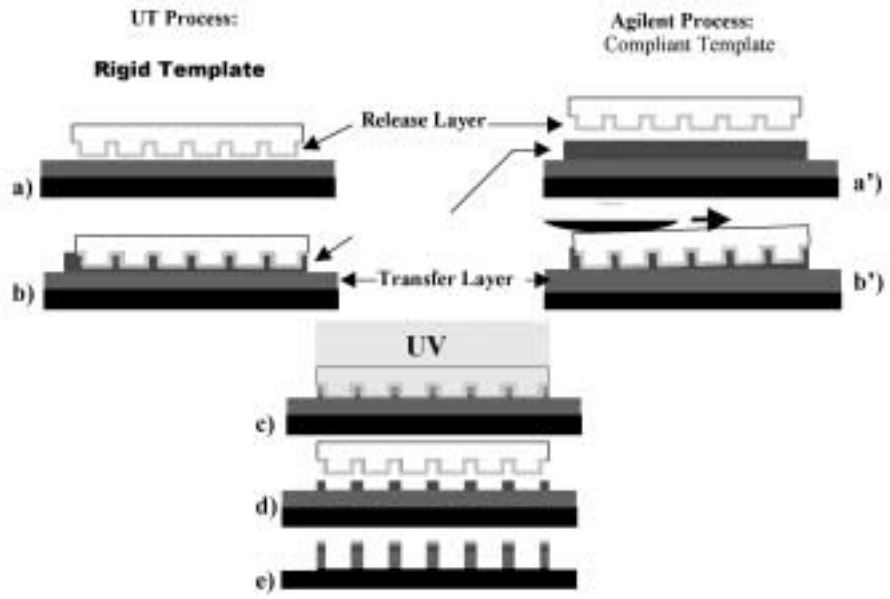

図2　二つのタイプのステップ･アンド･フラッシュ　インプリントリソグラフィ　プロセス（SFIL）。UTプロセスとAgilentプロセスはどちらも背面からUV照射が可能な透明なインプリントテンプレートと、低粘性で光ポリマー化するエッチ障壁用モノマー液を使用する。UTプロセスはテンプレート･基板目合わせ機構を備え硬いテンプレートと基板を平行に配置し(a)、その後エッチ障壁液を捕捉する(b)。圧力が十分強くなる薄い液層が排除されるとギャップは閉じる。Agilentプロセスではラミネーターローラーと柔軟性のあるテンプレートが使用され、余剰のエッチ障壁液を最大限押し出す(a ’とb ’)。背面から光照射し(c)エッチ障壁液を硬化する。テンプレートが引き上げられ(d)、高精度・低アスペクト比のエッチ障壁パターンが残される。余剰のエッチ障壁(ベース層)は短時間のハロゲンプラズマエッチングにより取り除かれ、その後、非等方的酸素エッチングによりパターンはトランスファ層に転写され(e)、高アスペクト比･高精度のパターンが作られる。この高アスペクト比構造はそのまま利用できるし、またはそれをエッチマスクとして使うこともできる。

Fig. 2　Two analogues of the Step and Flash Imprint Lithography Process. Both the UT process and the UT-Agilent process utilize transparent imprint templates to allow backside UV illumination, and they employ a low viscosity monomeric photopolymerizable etch barrier liquid. The UT process employs a template/substrate alignment scheme to bring a rigid template and substrate into parallelism (a), trapping the etch barrier (b). The gap is closed until the force that ensures a thin base layer is reached. The Agilent process utilizes a laminator roller and a compliant template to minimize the base layer (a’ and b’). The imprint is then illuminated through the backside of the template (c) to cure the etch barrier. The template is withdrawn (d), leaving low-aspect ratio, high resolution features in the etch barrier. The residual etch barrier (base layer) is etched away with a short halogen plasma etch, after which the pattern is transferred into the transfer layer with an anisotropic oxygen reactive ion etch (e), creating high-aspect ratio, high resolution features. These high aspect ratio features in the organic transfer layer can be utilized as-is, or can be used as an etch mask for transferring the features into the substrate.

engineering and materials science. We have begun to explore these challenges and report our progress here.

Careful tailoring of the chemistries allowed faithful replication of any feature on the imprint template. We have patterned 60 nm lines/spaces[4], areas of high and low pattern density, and produced a functional micropolarizer array with 100 nm Ti lines/spaces using a metal lift-off process[25]. SFIL has also been used to pattern directly over a non-flat substrate[25], including curved surfaces[26].

3.2 Advantages of Step and Flash Imprint Lithography

Within the realm of low cost imprint lithography, SFIL has several advantages over other imprint techniques. Other imprint techniques require a thermal cycle that is inherently slower than the UV illumination and the induced free radical polymerization. The thermal cycle also makes alignment difficult. To minimize thermal mismatch, many imprint techniques use identical materials for the template and substrate. Since typical substrates such as Si and GaAs are opaque in the visible range, this makes application of existing semiconductor manufacturing alignment schemes difficult. These materials are also brittle, creating an especially difficult task when separating molds created on semiconductor wafers from imprints created on similar substrates.

The low pressure, room temperature replication conditions used in SFIL provide the potential for layer-to-layer overlay alignment by: i) minimizing the force applied to the substrate-template interface hence minimizing material distortion of both the substrate and template, and ii) eliminating thermal expansion mismatch by patterning at room temperature. The ultraviolet and visible transparency of the template allows for application of existing overlay alignment techniques. An additional benefit is that these templates take advantage of existing reticle fabrication techniques and infrastructure as discussed below. The generation of high resolution, high aspect ratio features produced by SFIL and its multilayer resist scheme has yet to be demonstrated by other imprint techniques.

3.3 The Imprint Template

Imprint lithography is a 1-X pattern transfer process. The design and production of a high quality template is therefore key to its success. The templates are currently prepared following standard mask manufacturing techniques. A resist spin-coated on a chromium-coated quartz mask blank is patterned with an electron beam, and the exposed resist is developed away. The exposed chromium is removed through a dry etch process, after which the SiO_2 is etched using a standard phase-shift etch process, creating topography that is approximately 0.25 μm deep. The remaining chromium is then stripped, and 1-in. square templates are cut to fit the holder on our imprint apparatus. The 1-in. square template size was chosen because it represents a larger area than the maximum die size called for in the SIA Roadmap for Semiconductors[27]. Our most recent templates were produced at the Reticle Technology Center in Round Rock, Texas.

The ultimate resolution of imprint technologies is limited by the resolution of the imprint template or mold. It is therefore desirable to extend the ability of techniques used to pattern these templates to coincide with the SIA Roadmap for Semiconductors, which calls for 65 nm minimum resist feature size (for microprocessor gate length), and 130 nm minimum mask feature size (for optical proximity correction features) by 2005[27]. For the case of the 1-X pattern transfer in imprint lithography, the mask feature size targets need to be adjusted to coincide with the resist feature targets.

3.4 The Release Layer

Following exposure and curing of the photopolymer, during the SFIL process, ***Figure 2(c)***, the imprint template is drawn away from the substrate, ***2(d)***. In this step it is imperative that the etch barrier remain attached to the underlying transfer layer, and release easily and completely from the template. Consider a trench in the surface of the template with an aspect ratio of one. This trench creates a line of etch barrier. Three sides of the structure are in contact with the imprint template and one side is in contact with the transfer layer. If the surface energy of the template and transfer layer are equal, there is a high probability based on contact area considerations that the feature will adhere to the template and rip away from the substrate. The surface energy of the bare quartz template is actually higher than that of the transfer layer, leading to greater adhesive forces in the area of greater contact. It is therefore necessary to modify the surface energy of the template to promote selective release at the template-etch barrier interface.

There are two general types of release layers being considered by various research groups, deposited polymer films and self-assembling monolayer films. Jaszewski and coworkers have studied the reliability of deposited fluorocarbon films for use in hot embossing lithography[28, 29]. The authors conclude that functional fluorocarbon material

in the mold release layer becomes entrained in the imprinted material, thus limiting the lifetime of its mold release function[29]. With this in mind, we have focused on a fluorinated self-assembling monolayer release coating, which is described below.

Alkyltrichlorosilanes form covalent bonds with the surface of fused silica, or SiO_2, and can be used to modify the template surface energy. The -OH groups on the SiO_2 surface react with the silane to form HCl. The reaction of functional alkylsilanes with SiO_2 proceeds very slowly in the absence of surface water, but quite rapidly in the presence of surface water[30-33]. Tripp and Hair studied the reaction of alkykchlorosilanes and fluoroalkylchlorosilanes with silica using infrared spectroscopy, by monitoring the disappearance of glass surface SiO-H bond during the course of the reaction. They found that alkylsilanes do not react with a completely dehydrated surface, and the fluorinated counterparts do react, but slowly.

Alkyltrichlorosilanes react with surface bound water to form networks derived from the formation of bonds between adjacent molecules. The water adsorbed on the glass surface reacts with the self-assembled monolayer (SAM) precursor to form a silanol intermediate and an acid in an irreversible reaction[34]:

$$R\text{-}SiCl_3 + 3H_2O \rightarrow R\text{-}Si(OH)_3 + 3HCl$$

The intermediate has three -OH groups, which can either bond to the quartz surface or to adjacent molecules through the loss of water. This network formation makes it appealing for use as a durable release coating, and is shown in ***Figure 3***. Following the SAM formation, there may be some dangling -OH groups on the substrate surface as well as in the film. Tripp and Hair[35] have shown that post-formation annealing enhances the incorporation of these groups to form a more highly networked and highly bonded film.

Hare, *et al*.[36] predicted that a surface composed of only $-CF_3$ groups would have the lowest surface free energy of any system, at ~6 dynes/cm. Nishino, *et al*. later verified that prediction; their work on perfluorinated chains demonstrated a surface energy of 6.7 dynes/cm[37]. As a comparison, TEFLON® has a surface energy of 18 dynes/cm[38]. A good monolayer film with $-CF_3$ terminations has the potential to be a superb release coating for the SFIL template.

The surface treatment procedure used in the SFIL process is based on the information described above. The quartz templates were first cleaned with a piranha solution (1 part H_2O_2 to 2 parts H_2SO_4) for 30 minutes to remove any surface organic contaminants. After the piranha etch, the substrates were blown dry with N_2. The substrates were then heated to

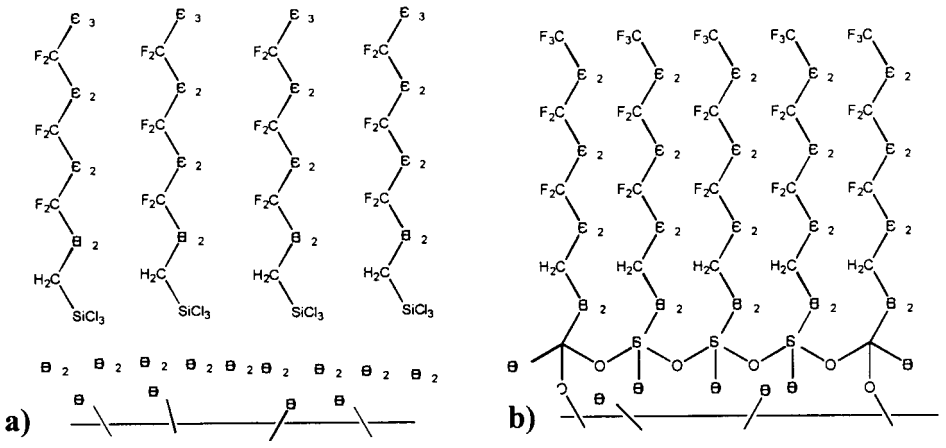

図3　テンプレートの表面処理手順。フッ素を含む自己組織化単層膜を使った低表面エネルギーコーティングをテンプレートに施し、硬化したエッチ障壁からテンプレートの切り離しを可能にする。トリクロロシランがテンプレートの表面にたどり着く(a)。そこで表面の水分と化合してシラノール中間体を形成する。これら中間体はクォーツ表面上のヒドロキシル類および隣り合うシラノールと縮合反応を起こし、ネットワークしたシロキサン単層膜を形成する(b)。この層はフロロアルカン鎖がクォーツから離れるように3次元の櫛状に配列する。さらにアニールすることにより凝縮が進み、高度にネットワークした耐久性のある低表面エネルギーのコーティングができる。

Fig. 3　Template surface treatment sequence. A fluorinated self-assembling monolayer is used to provide a low surface energy coating that ensures release of the cured etch barrier. Trichlorosilanes migrate to the template surface (a), where they react with surface water to form silanol intermediates. These intermediates undergo a condensation reaction with the hydroxyl groups on the quartz surface, as well as adjacent silanols, to form a networked siloxane monolayer (b). This layer is oriented such that the fluoroalkane chains are oriented away from the quartz, in a 3-D comb-like structure. Annealing further enhances the condensation, creating a highly networked, durable, low surface energy coating.

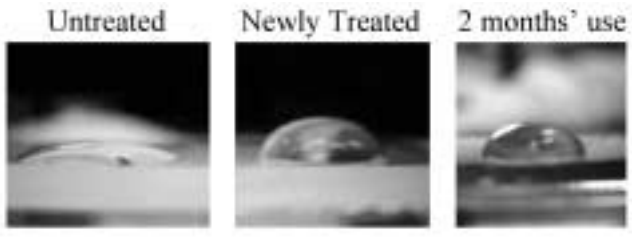

図4　表面処理の耐久性。表面処理は未処理のテンプレート(左)の表面エネルギーを下げ、撥水性の表面を作る(中)。水滴の接触角度には2ヶ月の使用後にも変化はない(右)。

Fig. 4 Surface Treatment Durability. The surface treatment lowers the surface energy of the untreated template (left), creating a hydrophobic surface (center). The water contact angle does not change significantly after two months' use (right).

90 ºC, and reacted with tridecafluoro-1,1,2,2,tetrahydrooctyl trichlorosilane (CF_3-$(CF_2)_5$-CH_2-CH_2-$SiCl_3$) [Gelest] for one hour.

The surface treatment reaction has yielded surface energies in the neighborhood of 12 dynes/cm. These surface energies do not approach the Zisman prediction, and we believe this is due to surface roughness effects which expose underlying -CF_2- groups. A surface composed of mixed -CF_3 and -CF_2 groups should have a surface energy in the range of 17 dynes/cm[38].

The surface treatment must maintain its release characteristics through hundreds or thousands of imprints in a manufacturing process. Preliminary results indicate that the current technique could provide films with the required durability. ***Figure 4*** shows the water contact angle on an untreated template (left), a newly treated template (center), and a treated template (right) that was used for a period of two months and was cleaned vigorously. The template retained its release functionality, and it can be seen that the water contact angle did not change significantly. We have seen no evidence of catastrophic loss of release function. Work is currently underway to quantify film durability for a variety of treatment conditions.

3.5 The Etch Barrier

3.5.1 Chemical Property Criteria

Several critical issues must be considered in designing the SFIL etch barrier chemistry including adhesion, photopolymerization kinetics, shrinkage, and etch selectivity. Tailoring surface properties is crucial. The etch barrier fluid must wet the template well to facilitate filling of the topography, yet it must release from the template readily after exposure. These requirements are conflicting, and the trade-offs must be analyzed and understood.

3.5.2 Chemical Formulations

We formulated our first etch barrier solutions from a free radical generator dissolved in a solution of organic monomer, silylated monomer, and a dimethyl siloxane (DMS) oligomer. Each component serves a specific role in meeting these constraints. The free radical generator initiates polymerization upon exposure to actinic illumination. The organic monomer ensures adequate solubility of the free radical generator and adhesion to the organic transfer layer. The silylated monomers and the DMS provide the silicon required to give a high oxygen etch resistance. Both monomer types help maintain the low viscosity required for filling. The silylated monomer and DMS derivative also serve to lower the surface energy, allowing for template release.

Test formulations were made from a variety of commercially available monomers and DMS derivatives listed in ***Table 1***. These were tested for reactivity and surface energy properties over the range of concentrations listed. The silylated monomers, crosslinking agents, and DMS derivatives were purchased from Gelest, Inc., and used as received. The free radical generators were acquired from Ciba-Giegy Specialty Chemicals Division. The organic

Table 1 Components and Range of Compositions Tested as Viable Etch Barrier Solution

Principal Component	Weight %	Chemical Names
Monomer	25-50	Butyl acylrate, methyl acrylate, methyl methacrylate
Silylated monomer	25-50	Methacryloxypropyl tris(trimethylsiloxy) silane (3-Acryloxypropyl) tris(tri-methylsiloxy) silane
Dimethyl siloxane deriviative	0-50	(Acryloxypropyl) methylsiloxane dimethylsiloxane copolymer (Acryloxypropyl) methylsiloxane homopolymer Acryloxy-terminated polydimethylsiloxane
Crosslinking agent	0-5	1,3-Bis(3-methacryloxypropyl)-tetramethyl disiloxane
Free radical generator	2-10	Irgacure 184, Irgacure 819

monomers were purchased from Aldrich. A statistical response surface optimization procedure was employed to develop the preliminary etch barrier formulations.

3.5.3 Photopolymerization Kinetics

High productivity with SFIL will require rapid photopolymerization of the etch barrier. We have therefore set out to establish methods of directly measuring photopolymerization kinetics and will expand these studies to include the time evolution of mechanical properties and surface energy. We have conducted preliminary studies on the kinetics of the photopolymerization curing process using real-time infrared spectroscopy. In this method, the IR absorbance of the polymerizing functional group is monitored while the sample is simultaneously exposed to UV irradiation. As polymerization proceeds, the concentration, and thus absorbance, of the polymerizing functional group decreases. Several variations on this experimental method are described in the literature[39-41], and the specific experimental procedure we used is described in a previous publication[4].

The ideal etch barrier should polymerize quickly and achieve nearly total conversion of the polymerizing functional group. Our kinetic experiments showed that the etch barrier components we auditioned varied widely in their rate of polymerization. Variation in extent of conversion among the components was also observed. ***Figure 5*** shows photocuring data for organic and silylated monomers. Of the organic monomers, butyl acrylate and methyl acrylate are both viable candidates for inclusion in the etch barrier solution, but methyl methacrylate clearly is not; the rate of methyl methacrylate polymerization is much too slow to achieve high conversion in a reasonable exposure time. ***Figure 5*** also shows that butyl acrylate and methyl acrylate both achieve close to total conversion. Hence, our first fluid formulations were based on acrylates. The cure rates for silylated monomers showed a pattern similar to the organic monomers. The cure rate for the acryloxysilane monomer was much greater than that for the methacryloxysilane monomer.

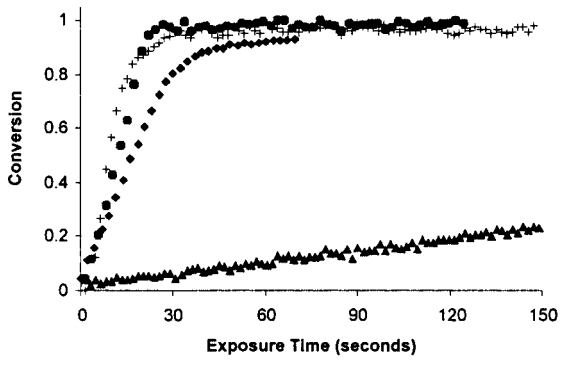

図5　有機およびシリル化したアクリル酸モノマーの光ポリマー化効率。アクリル酸ブチルButyl acrylate (◆)、アクリル酸メチルmethyl acrylate (●)、メタクリル酸メチルmethyl methacrylate (▲)、アクリオキシシランacryloxy silane (+)、メタクリオキシシランmethacryloxysilane (□)。

Fig. 5. Organic and Silylated Acrylate Monomer Photopolymerization Rates. Butyl acrylate (◆), methyl acrylate (●) methyl methacrylate (▲), acryloxysilane (+), methacryloxysilane (□)

Based on these results, our first pass etch barrier formulation consisted of 47 wt.% UMS-182, 3.5 wt.% Irgacure 184, 1.5 wt.% Irgacure 819, 24 wt.% SIA 0210.0, and 24 wt.% butyl acrylate. We use approximately one microliter of etch barrier for each 1 square inch imprint.

3.6 The Transfer Layer

The transfer layer is an organic film that can vary in thickness with specific application, but must follow certain guidelines. The transfer layer should not be soluble in the liquid etch barrier, and must adhere well to the cured etch barrier. The transfer layer must remain intact after exposure. There should be at least modest etch selectivity between the etch barrier and the transfer layer to obtain aspect ratio magnification. These and other issues are being considered as materials development continues.

We are currently using PMMA and HR100 [Olin] as transfer layer materials. The etch barrier solution is a mixture of acrylate monomers and co-monomers containing a percentage of silicon. This silicon content provides the etch selectivity between the etch barrier and transfer layer that allows amplification of the aspect ratio during oxygen reactive ion etch. The development and selection of the optimum transfer layer materials is ongoing. The transfer layer used in early studies was poly(methyl methacrylate) (PMMA) (967k MW), spun at 3k rpm from a 2.5% solution in chlorobenzene, then baked at 180 ºC for a minimum of 4 hours to yield films ~200 nm thick.

3.7 The Equipment

Imprint lithography relies on the parallel orientation of the imprint template and the substrate. Inaccurate orientation may yield a layer of cured etch barrier that is non-uniform across the imprint field, and attempts to amplify the aspect ratios of the imprinted image may only amplify this non-parallel effect. It was therefore necessary to develop a mechanical system whereby the template and substrate are

brought into co-parallelism during etch barrier exposure.

This is achieved in SFIL by way of a two step orientation scheme. The first step is an active, user-controlled, global or wafer-scale orientation, wherein the template stage holder and wafer chuck are rotated about the α and β axes to bring the two surfaces into approximate parallelism, and is shown schematically in ***Figure 6***. ***Figure 6a*** represents an improperly aligned system. The flexure stages, one each placed below the wafer chuck and above the template stage, allow one translation motion (z displacement) and two tilting motions (α and β rotation), ***Figure 6b***. The passive, fine orientation stage affects the system during imprinting to achieve perfectly uniform surface contact between the template and substrate, ***Figure 6c***.

Figure 7a shows an ideal kinematic stage composed of perfect rigid bodies and joints. The ideal kinematic stage has several practical limitations with respect to SFIL process. Presence of sliding contacts in joints can cause wear, generate undesirable particles and lead to stiction that makes precision motion control difficult. Presence of clearances in joints can lead to reduced repeatability in the motion of the mechanism. Flexures generate motion by elastic deformation, avoid all the problems associated with joints, and are becoming quite common in the precision engineering industry[42, 43]. Multiple imprints are performed by moving an 8" wafer to various x-y positions while holding a template stationary. For the multi-imprint process, it is necessary to have the compliant flexure affixed to the template since a rigid template and compliant wafer stage can lead to an unstable configuration for imprinting away from the center of the substrate[43]. The orientation stage design that can tilt a template about the two "remote axes" that lie on the template-wafer interface (one of them denoted as "C" in ***Figure 7b***) was developed and described

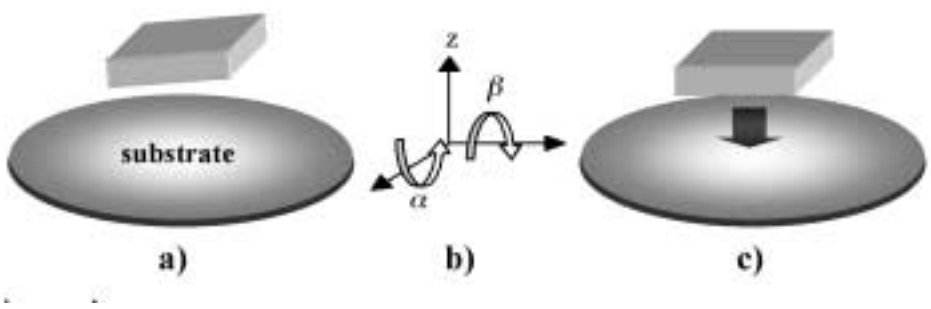

図6　不適当な方位に配置されたテンプレート・基板システム(a)、望ましい目合わせ動作の方位調整の自由度 (b)、そして適切に方位が調整されインプリント準備ができたシステム(c)。SFILの方位調整には二つの仕組みが組み込まれている。能動的で粗い方位調整はウエファー全体の平行性調整を行い、受動的で微細な方位調整は局所的な目合わせを行う。

Fig. 6　Improperly oriented template and substrate system (a), desired orientation alignment motions (b), and properly oriented system ready for imprinting (c). The SFIL orientation scheme incorporates both an active, course orientation that is used to correct global, or wafer-scale parallelism issues, and a passive, fine orientation that minimizes local misorientation.

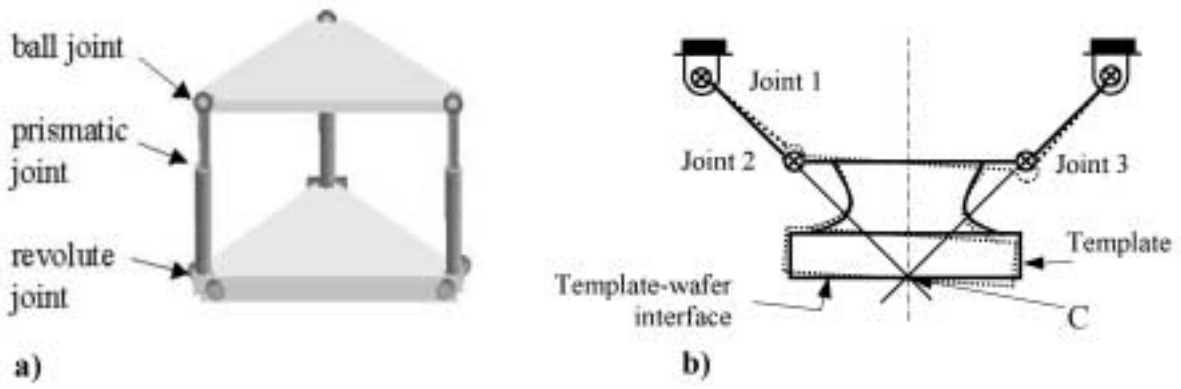

図7　受動的な方位調整の仕組み。理想的な剛体による動的モデル(a)では適切な自由度（αとβの回転とzの平行移動）が確保される。実際のテンプレート台の設計(b)では、すべて「たわみジョイント」(flexure joints)が使用されているので、自由度の制約に従って方位調整ができる。SFILでは(b)図のような一方向軸の設計を、すでに二方向軸のものに発展させている。

Fig. 7　The passive orientation scheme. Ideal kinematic model (a), which allows the proper degrees of freedom, α and β rotation, and z translation. Single axis template stage design (b), using only flexure joints, which complies to the DOF constraints. This design has been extended to a two-axis design for SFIL.

elsewhere[43]. Two flexures are mounted orthogonal to each other in order to generate two tilting motions, about the α and β axes.

A multi-imprint Step and Flash Lithography machine that can perform repeated imprints on 200 mm wafers was developed for the purpose of defect analysis, and is shown in a previous publication[44]. This machine can imprint high resolution (sub 100 nm) features from quartz templates using a step and repeat process. The major machine components include the following: (i) a micro-resolution Z-stage that controls the average distance between the template and the substrate and the imprinting force; (ii) an automated X-Y stage for step and repeat positioning; (iii) a pre-calibration stage that enables attainment of parallel alignment between the template and substrate by compensating for orientation errors introduced during template installation; (iv) a fine-orientation flexure stage that provides a highly accurate, automatic parallel alignment of the template and wafer to the order of tens of nanometers across an inch[43]; (v) a flexure-based wafer calibration stage that orients the top of the wafer surface parallel with respect to the plane of the XY-stage; (vi) an exposure source that is used to cure the etch barrier; (vii) an automated fluid delivery system that accurately dispenses known amounts of the liquid etch barrier; and (viii) load cells that provide both imprinting and separation force data.

The multi-imprint apparatus is currently configured to handle 1-in. square templates. It is used to produce more than 20 imprints on 200mm wafers for defect studies. The installation of the template and the loading and unloading of the wafer are performed manually. The printing operations, including X-Y positioning of the wafer, dispensing of etch barrier liquid, translation of the template to close the gap between the template and wafer, UV curing of etch barrier, and controlled separation are all automated. These unit processes are controlled by a LabVIEW® interface. Detailed information about the major subcomponents of the system is available in a previous publication by this group[43].

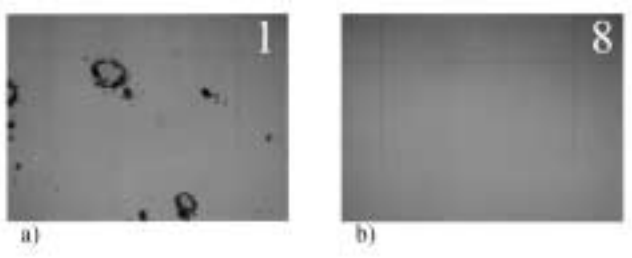

図8　テンプレートに起因するコンタミネーションの消失がこの写真で見える。(a)は最初のインプリントの顕微鏡写真である。大きな欠陥もインプリントを繰り返すうちに減少し、8回目のインプリントでは完全に消失している(b)。

Fig. 8 The disappearance of template-bound contamination can be seen in these images. Image 1 is a micrograph of the first imprint, and even the very large defects shrink upon successive imprinting and completely disappear after the eighth imprint.

3.8 Defects?

Imprint lithography skeptics insist that this type of contact patterning will necessarily create defects in the resulting pattern. A study is underway to investigate creation and propagation of defects in SFIL. The process defects one may encounter in contact patterning may be divided into groups (neglecting template generation defects): (i) particles or contaminants that originate on the imprint template; (ii) bubbles formed during the etch barrier displacement; and (iii) pattern defects caused by features adhering to the template and pulling away from the substrate. Type (i) defects are discussed below. It can be shown, although it is not done so here, that type (ii) defects are not seen with low viscosity etch barrier solutions, even at very high resolution features. We generally do not seen type (iii), as long as the surface treatment and etch barrier are prepared according to specification.

Wafers with multiple imprints were carefully analyzed for defects. One region of the imprint field was tracked through multiple imprints starting with the first imprint using an Olympus microscope. The size of the defects was estimated and tracked (not shown). ***Figure 8(a)*** shows a field of severe defects, some of which are identified for tracking purposes. These defects were followed through consecutive imprints. After eight imprints, the region was free of defects, as seen in ***Figure 8(b)***. We believe that the defects are removed by entrainment in the etch barrier, thus cleaning the template for the following imprints. Based on these results, it appears that the process is self-cleaning for contaminants on the template.

4 Imprinted Features

We have used the process flow shown on the left side of ***Fig. 2*** in much of our process development. We have also collaborated with Agilent Technologies, which afforded us with the opportunity to perform some fundamental work in implementation of the technology. The UT-Agilent collaboration used a variation on the SFIL process flow described in Section 3.1. This variation employed a roller

imprint technique similar to that used by Tan, *et al*.[45], but which incorporated the preferred UV-curable/organic bilayer resist scheme. The UT-Agilent process flow is shown in the right side of ***Figure 2***, alongside the primary SFIL process flow.

Figure 9 is an SEM image of a grating structure patterned in etch barrier. Using a wafer with 80 nm features replicated on 1.1 microns of hard-baked PMMA, the O_2 RIE was halted after partially penetrating the PMMA layer (approx. 300 nm), shown in ***Figure 9(a)***. After determining the features could structurally withstand such high aspect ratio, another section of the same wafer was etched until the endpoint was determined by HeNe interferometry. This sample was also characterized by SEM and is shown in ***Figure 9(b)***, which is a top-down view. These features have a remarkable aspect ratio of 14:1, and demonstrate a benefit of the multilayer resist scheme used by SFIL.

A high-resolution template with an array of orthogonal 100 nm lines/spaces (L/S) was used to create a micropolarizer array. Following imprinting and etch transfer, Ti was deposited at a rate of 2.5 nm/s in a metal evaporator. The substrate was immersed in an ultrasonic bath of acetone to remove the resist features, leaving the Ti that was adhered to the substrate. The result was an alternating array of orthogonal micropolarizers shown in ***Figure 10***. ***Figure 10(a)*** is a close-up SEM of the lines/spaces in the image, and ***Figure 10(b)*** is the array illuminated with polarized light. The optical micrograph in ***Figure 10(b)*** is a bit deceiving,

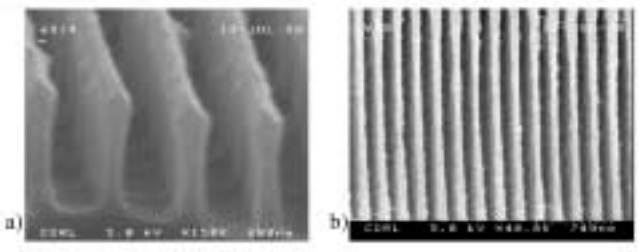

図9　(a)“ Etch and Stop ”実験の結果では、200nmピッチの80nmラインが1.1ミクロンのPMMA層に部分的に転写されている。(b)上から見た写真ではこの構造がPMMA全体に転写されているのがわかる。アスペクト比は約14対1である。ライン側面の粗さは、ベース層（余剰のエッチ障壁）を通してのエッチングが不完全であったことによる。

Fig. 9　a) 80nm lines on 200nm pitch transferred partially through a 1.1 micron layer of PMMA in an “Etch-Stop” experiment. b) Top-down view of these features transferred through the entire PMMA layer, yielding aspect ratios nearly 14:1. The line edge roughness is an artifact of an incomplete etch through the base layer.

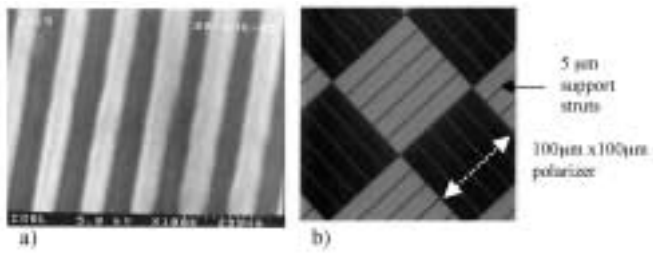

図10　リフトオフ法で作られた100nmのチタン線の電子顕微鏡写真(a)。マイクロ偏光器アレーを偏光光で照射した光学顕微鏡写真(b)。

Fig. 10　SEM close-up of 100 nm Ti lines patterned with metal lift-off techniques (a). Optical micrograph of a micropolarizer array illuminated with polarized light (b).

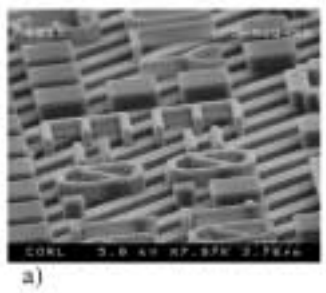

図11　平坦化をした有機平坦化層に250nmの構造を転写することができる。

Fig. 11　250nm feature transferred through the planarizing organic layer.

the thin lines in the square regions are actually perpendicular to the direction of Ti lines in that region, and serve to support the lines. It was thought that 100 nm resist lines at the aspect ratios used for the metal lift-off process would collapse if designed to extend the entire width of the 100 micron square. The polarization ratio for the device was measured to be between 5:1 and 10:1, but could be improved by redesign of these support struts.

The ultimate goal of the Agilent collaboration was to pattern a non-flat substrate with imprint lithography. Starting with a pre-patterned substrate, typically a silicon wafer with either a Fresnel lens or hologram etched 700 nm deep into silicon, PMMA (497,000 MW) was spun at 6000 RPM to provide a thin organic layer. Then, a planarization layer of a pure organic solution was photopolymerized over the hard baked PMMA using a non-patterned imprint. Finally, the etch barrier was patterned over the planarized organic layer. High aspect ratio resist features such as those shown in ***Figure 11*** were generated using the same etch transfer process as that used for flat substrates. Features as small as 250 nm were etched over the 700 nm topography.

5. Conclusions

Step and Flash Imprint Lithography appears to have several process advantages over comparable compression imprinting techniques. Step and Flash Imprint Lithography is capable of high resolution patterning at room temperature with ~14 kPa applied pressure. SFIL utilizes chemicals that are commercially available to pattern in the sub-100 nm regime. The completion of the SFIL stepper marks the first step toward imprint lithography with the possibility of high-resolution layer-to-layer alignment. The Step and Flash multilayer scheme has been successfully applied to the patterning of 60 nm lines with 6:1 aspect ratio (not shown here) and 80 nm features with 14:1 aspect ratio. Using metal lift-off, we have successfully patterned 100 nm metal lines/spaces and generated a functional micropolarizer array. Exploiting the high aspect ratio patterning of SFIL's multilayer scheme, 250 nm features were patterned over 700 nm topography.

An automated tool for Step and Flash Imprint Lithography has been constructed. This tool allows an operator to run automated imprinting experiments without human intervention, except for installation of templates, and loading and unloading of wafers. Imprint templates were treated with a low surface energy self-assembled monolayer to aid selective release at the template-etch barrier interface. This surface treatment was shown to be quite durable, surviving repeated imprints and multiple aggressive physical cleanings without loss of function.

The SFIL process appears to be “self-cleaning.” The number and size of imprinted defects resulting from template contamination decreased with each successive imprint. The imprint field was contamination free after 8 imprints. Contamination on the template was observed to be entrained in the polymerized etch barrier.

ACKNOWLEDGEMENTS

We thank DPI-RTC, International SEMATECH, and Compugraphics for generous gifts and technical consultation to the project. Special thanks to Franklin Kalk, Cece Philbin, and Ric Diola for help in getting imprint templates, and Dan Felder for his help in defect analysis. We would like to thank all those at Agilent Laboratories for all their assistance especially Judith Seeger, Karen Seaward, and Jim Krugger. We gratefully acknowledge the financial support of DARPA (MDA972-97-1-0010) and SRC (96-LC-460).

References

1) *3rd International SEMATECH Next Generation Lithography Workshop*. 1999: CO.
2) Thompson, L.F. and C.G. Willson, eds. *Introduction to Microlithography*. M.J. Bowden, ed.. 1994, ACS: Washington, D.C. p. 70.
3) Chou, S.Y., P.R. Krauss, and P.J. Renstrom. J. Vac. Sci. Tech. B, **14**(6) (1996) 4129.
4) Colburn, M., *et al*. in *SPIE's 24th International Symposium on Microlithography: Emerging Lithographic Technologies III*. 1999. Santa Clara, CA, **3676(I)**, p. 379.
5) Haisma, J., *et al*. J. Vac. Sci. Tech. B, **14**(6) (1996) 4124.
6) Xia, Y. and G.M. Whitesides. Angew. Chem. Int. Ed. Engl., **37** (1998) 550.
7) Jaszewski, R.W., *et al*. Microelectronic Engineering, **41/42** (1998) 575.
8) Scheer, H.-C., *et al*. in *Electron, Ion and Photon Beam Technol. and Nanofabrication*. 1998. Chicago.
9) Chou, S.Y., *http://www.ee.princeton.edu/~chouweb/newproject/page3.html*.
10) Chou, S.Y., P.R. Krauss, and P.J. Renstrom. Appl. Phys. Lett., **67**(21) (1995) 3114.
11) Chou, S.Y., P.R. Krauss, and L.Kong. J. Appl. Phys., **79**(8) (1996) 6101.
12) Krauss, P.R. and S.Y. Chou. Appl. Phys. Lett., **71**(21) (1997) 3174.
13) Wang, J., *et al*. J. Vac. Sci. Tech. B, **17**(6) (1999) 2957.
14) Yu, Z., S.J. Schablitsky, and S.Y. Chou. Appl. Phys. Lett., **74**(16) (1999) 2381.
15) Wang, J., *et al*. Applied Physics Letters, **75**(18) (1999) 2767.
16) Guo, L., P.R. Krauss, and S.Y. Chou. Appl. Phys. Lett., **71**(13) (1997) 1881.
17) Guo, L., E. Leobandung, and S.Y. Chou. Science, **275**(5300) (1997) 649.
18) Schultz, H., *et al*. J. Vac. Sci. Tech. B, **18**(4) (2000) 1861.
19) Li, M., *et al*. in *Electron, Ion and Photon Beam Technol. and Nanofabrication*. 2000. Palms Springs ,CA.
20) Zhang, W. and S.Y. Chou. in *Electron, Ion and Photon Beam Technol. and Nanofabrication*. Palms Springs,CA.
21) Shaw, J., *et al*. Solid State Technology, **30**(6) (1987) 83.
22) Bouwhuis, G., *et al., Principles of Optical Disc Systems*. 1985, Bristol: Adam Hilger.
23) Wang, D., *et al*. Appl. Phys. Lett., **70**(12) (1997) 1593.
24) Widden, T.K., *et al*. Nanotechnology, **7** (1996) 447.
25) Colburn, M., *et al*. in *SPIE's 25th Intl. Symp. Microlithography: Emerging Lithographic Technologies IV*. 2000. Santa Clara, CA, **3997**, p. 453.
26) Ruchoeft, P., *et al*. J. Vac. Sci. Tech. B, **17**(6) (1999) 2965.
27) SIA, *International Technology Roadmap for*

Semiconductors: Lithography. 1999.
28) Jaszewski, R.W., *et al*. Microelectronic Engineering, **35** (1997) 381.
29) Jaszewski, R.W., *et al*. Applied Surface Science, **143** (1999) 301.
30) Zhao, X. and R. Kopelman. J. Phys. Chem., **100** (1996) 11014.
31) Silberzan, P., *et al*. Langmuir, **7** (1991) 1647.
32) Le Grange, J.D. and J.L. Markham. Langmuir, **9** (1993) 1749.
33) Tripp, C.P., R.P.N. Veregin, and M.L. Hair. Langmuir, **9** (1993) 3518.
34) Tripp, C.P. and M.L. Hair. Langmuir, **11** (1995) 1215.
35) Tripp, C.P. and M.L. Hair. Langmuir, **11** (1995) 149.
36) Hare, E.F., E.G. Shafrin, and W.A. Zisman. J. Phys Chem., **58** (1954) 236.
37) Nishino, T., *et al*. Langmuir, **15** (1999) 4321.
38) Ulman, A., *An Introduction to Ultrathin Organic Films from Langmuir-Blodgett to Self-Assembly*. 1991, Boston: Academic Press. p. 442.
39) Chiou, B.-S. and S.A. Khan. Macromolecules, **30**(23) (1997) 7322.
40) Crivello, J.V., T.L. Lai, and R. Malik. J. Polym. Sci. A: Polym. Chem., **34**(3103) (1996).
41) Decker, C. and M. K. J. Coatings Tech., **62**(786) (1990) 55.
42) Smith, S. and D.G. Chetwynd, *Foundations of Ultraprecision Mechanism Design*. 1992, Philadelphia: Gordon and Breach Science Publishers.
43) Choi, B.J., *et al*. in *ASME DETC2000/MECH-14145*. 2000. Baltimore, MD,
44) Bailey, T., *et al*. J. Vac. Sci. Tech. B, (2000) [submitted].
45) Tan, H., A. Gilbertson, and S.Y. Chou. J. Vac. Sci. Tech. B, **16**(6) (1998) 3926.

Todd C. Bailey

Todd C. Bailey is a University of Texas at Austin College of Engineering Thrust Fellow, and is pursuing his Ph.D. in chemical engineering. He earned his A.S. at Hudson Valley Community College in 1996, and S.B. at the Massachusetts Institute of Technology in 1998. His research interests include electronics materials chemistry, thin film growth kinetics and chemistry, and interfacial phenomena.

Byung Jin Choi

Byung Jin Choi is a post-doctorate fellow at the University of Texas at Austin. He earned his Ph.D. in mechanical engineering at UT Austin in 1998, with a specialty in mechanical system and design, and his B.S. at Hanyang University in Seoul in 199 1 . He joined the SFIL research group in 1998 and has been involved in imprint machine and process development. His research interests include ultra high precision machine development, flexure mechanism design and control, and planar and spatial kinematics.

Matthew Colburn

Matthew Colburn is Richard W. Moncrief Endowed Graduate Fellow and a University of Texas at Austin Graduate Fellow, and is pursuing his Ph.D. in chemical engineering. He earned his M.S. at UT Austin in 2000, and his B.S. at Purdue University in 1996. His research interests include alternative lithography development.

[no photo available]

Annette Grot

Annette Grot is currently project manager of the nanoscale photonics group at Agilent Technologies' central research facility in Palo Alto, California. She received her Ph.D. at the California Institute of Technology in electrical engineering in 1994. Her main research interests are in optical interconnects, diffractive optical elements and optoelectronic integrated circuits.

Mario J. Meissl

Mario J. Meissl is pursuing his B.S. in Mechanical Engineering at The University of Texas at Austin. He earned an A.S. in engineering from Central Texas College in 1997. He joined the SFIL team in February 1999 as an Undergraduate Research Assistant and serves as CAD Modeling and Finite Element Analysis support for various projects in the group. He is interested in modeling mechanical systems, mechanism design, and precision engineering.

Michael Stewart

Michael Stewart is an AMD/SRC Research Fellow, and is pursuing his Ph.D. in chemical engineering at the University of Texas at Austin. He earned his B.S. in chemical engineering at Vanderbilt University in 1998. His research interests include acid transport in photoresist.

John G. Ekerdt

John G. Ekerdt is the Z. D. Bonner Professor in Chemical Engineering and Department Chair. He earned his B.S. at the University of Wisconsin in 1974, and Ph.D. at the University of California at Berkeley in 1979. His research focuses on electronic materials chemistry; thin film growth kinetics and chemistry, nanostructured materials, compound semiconductor materials, silicon-alloy materials, barrier materials, and functional polymer films.

Dr. Sreenivasan

Dr. Sreenivasan is Associate Professor in Mechanical Engineering at UT Austin. He specializes in developing analytical and experimental tools for understanding kinematics and dynamics of machine systems, and applies these tools to the design and control of novel robotic devices. He has ongoing research in the area of micro and nano-resolution imprint lithography machines, macro-motion precision machines based on flexures, partially constrained compliant tables, and optical sensor architectures for on-line decision making and control. He is also involved in the development of robotic devices for hazardous environments, and the design of semi-autonomous off-road robotic vehicles.

C. Grant Willson

C. Grant Willson is a Professor of Chemistry and Chemical Engineering and holder of the Rashid Engineering Regents Chair at the University of Texas at Austin. He received his B.S. and Ph.D. degrees from the University of California at Berkeley and an M.S. degree from San Diego State University. He is a member of the National Academy of Engineering and has received numerous awards for his contributions to polymer chemistry and the design of organic materials for microelectronics.

ダイレクトトンネルメモリ(DTM)の展望

二木俊郎　臼杵達哉　堀口直人　(株)富士通研究所

Current status and prospects of direct tunneling memories(DTMs)

T. Futatsugi, T. Usuki, N. Horiguchi　*Fujitsu Laboratories Ltd.*

A novel floating gate memory, Direct Tunneling Memory (DTM), is demonstrated for embedded applications. This memory makes use of an ultra thin tunnel oxide to transfer electrons from and into a floating gate by direct tunneling, resulting in high speed write/erase operation with low voltage. The leakage current from floating gate is suppressed and long retention time is achieved by introducing a sidewall control gate structure, which spatially separates the floating gate from source/drain extensions. DTM requires neither new material nor complicated structure. Manufacturing process of DTM is highly compatible with that of logic circuits.

1．はじめに

メモリとロジックの混載技術は、電子機器の小型化、高速化、低消費電力化を同時に達成する技術として期待されている。特に、大容量で高速なＤＲＡＭ(Dynamic Random Access Memory)と高性能ロジックを混載させる技術に対するニーズは高い。しかし、DRAMのセルに用いられるキャパシタは、微細化が進みセルサイズが小さくなっても、ある程度の容量(～30fF)を確保する必要があるため、近年のキャパシタの構造は複雑化しており、さらに、従来は用いられなかった高誘電体材料やそれに伴う新しい電極材料の導入が進められている。メモリとロジックを混載したシステムLSIを低コストで実現するためには、このような